Combination of Metal−Metal Bonding and Antiferromagnetic Exchange Interaction in the d^2-d^2 Complex [V₂O(SPh)₄(Me₂-bpy)₂]·THF (Me₂-bpy = 4,4′-Dimethylbipyridine)

Norman S. Dean, Stuart L. Bartley,[†] William E. Streib, Emil B. Lobkovsky, and George Christou*

Department of Chemistry and Molecular Structure Center, Indiana University, Bloomington, Indiana 47405

Synthetic procedures leading to the preparation of V^III and V^IV complexes of PhS⁻ are described, including the mononuclear complex (NEt₄)[V(SPh)₄(bpy)] (1). Controlled aerial oxidation of its 4,4′-Me₂-bpy (Me₂-bpy) analogue generated *in situ* with 0.5 equiv of O₂ leads to generation of [VO(SPh)₃(Me₂-bpy)]⁻ that can be isolated as the NR₄⁺ salts; (NMe₄)[VO(SPh)₃(Me₂-bpy)] (2) has been structurally characterized and contains a distorted-octahedral anion with three equatorial PhS⁻ groups and one Me₂-bpy N atom of the chelate *trans* to the multiply-bonded O atom. Crystal data for **2**: monoclinic, C2/c, a = 28.618(5) Å, b = 10.053(1) Å, c = 24.194(3) Å, β = 113.40-(1)°, Z = 8, T = −157 °C, and V = 6387.8 Å³; R (R_w) = 5.85 (5.81)% for 3306 unique reflections with $F > 3\sigma(F)$. The same oxidation reaction with the related ion [V(SPh)₂(bpy)₂]⁺ leads to [VO(SPh)(bpy)₂](PF₆) (3). Controlled hydrolysis of [V(SPh)₄(Me₂-bpy)]⁻, generated *in situ*, leads to isolation of V₂O(SPh)₄(Me₂-bpy)₂ (4) which has a [V₂(μ-O)(μ-SPh)₂]²⁺ core with a terminal PhS⁻ and chelating Me₂-bpy on each metal; the V−V separation of 2.579(3) Å is suggestive of a V^III−V^III single bond. Crystal data for **4**: monoclinic, C2/c, a = 16.954(3) Å, b = 15.969(2) Å, c = 18.830(3) Å, β = 107.96(1)°, Z = 4, T = −173 °C, and V = 4849.5 Å³; R (R_w) = 6.44 (6.46)% for 2115 unique reflections with $F > 3\sigma(F)$. EHT calculations on the model complex V₂O(SH)₄(NH₃)₄ indicate a V−V σ bond arising from V d_{z^2} overlap, with the HOMO and LUMO comprising δ and δ* orbitals, respectively, formed by V d_{xy} orbitals. A small HOMO−LUMO gap (∼0.02 eV) suggests the weak room-temperature paramagnetism is due to thermal population of the LUMO. Variable-temperature solid-state studies on **4** indicate an effective magnetic moment per dimer (μ_{eff}/V_2) of 1.35 μ_B at 330 K decreasing to 0.095 μ_B at 5.0 K. The data were fit to the Bleaney−Bowers equation for a d¹−d¹ dimer, and the obtained parameters were J = −355 ± 20 cm⁻¹, g = 2.04, and TIP = 300 × 10⁻⁶ cm³ mol⁻¹ with a 1.4% paramagnetic (V^III) impurity. Variable-temperature ¹H NMR studies on complex **4** in d_8-THF solution in the −90 to +50 °C range were fit to the appropriate equation relating the ¹H paramagnetic shifts to a number of parameters including J. The obtained value of J for **4** in solution was −280 ± 20 cm⁻¹. The calculated singlet−triplet gaps for **4** are $|2J|$ = 710 and 560 cm⁻¹ for the solid and solution phases, respectively.

Introduction

During the last several years, we have been involved in developing non-organometallic vanadium/sulfur chemistry, an area that was, and still is, relatively unexplored compared with molybdenum/sulfur chemistry. Our interest in this field stems from the frequent occurrence of large amounts of vanadyl [VO]²⁺ impurities in crude petroleum, and the deleterious consequences these (and to a lesser extent other) metal impurities have on the heterogeneous hydroprocessing catalyst, i.e., the supported Mo catalyst that effects hydrodesulfurization (HDS) and hydrodenitrification (HDN).[1−3] Under the high temperatures (∼350−400 °C), reducing conditions (H₂), and sulfur-rich (generated H₂S) conditions of the refining process, hydro-

demetal(iz)ation (HDM) of the vanadyl impurities occurs, leading to formation of black, insoluble V sulfides (mainly V₂S₃ and V₃S₄) that deposit on the Mo catalyst and decrease its activity, eventually causing total deactivation by pore-plugging.[1−3]

The overall transformation of crude oil V impurities from mononuclear vanadyl (V^IV) species (porphyrins and a variety of non-porphyrins) to polymeric V₂S₃ and V₃S₄ (V^II, V^III) solids is poorly understood, particularly with respect to any discrete V/S species that may be intermediates in this process. Thus, we have sought to contribute to this area by preparing V/O and V/S oligonuclear species that may be intermediates in the initial and later stages, respectively, of the [VO]²⁺ to V₂S₃/V₃S₄ conversion and characterizing them by a number of spectroscopic and physicochemical techniques. Over the last several years, we have reported a number of such V species, spanning the oxidation states II−V, including mixed-valency, and the metal nuclearities 1−6.[4,5] To date, our V thiolate work has primarily employed the chelate 1,2-ethanedithiolate (edt²⁻), which has proven beneficial in preventing formation of insoluble polymers.

† Department of Chemistry, Michigan State University.
⊗ Abstract published in *Advance ACS Abstracts*, March 1, 1995.
(1) (a) Speight, J. G. *The Chemistry and Technology of Petroleum, Chemical Industries*, 3; Marcel Dekker, Inc.: New York, 1980. (b) Yen, T. F. In *The Role of Trace Metals in Petroleum* Ann Arbor Science: Ann Arbor, MI, 1975; Chapter 1.
(2) (a) Psundararaman, P. *Anal. Chem.* **1986**, *57*, 2204. (b) Reynolds, J. G.; Gallegos, E. J.; Fish, R. H.; Komlenic, J. J. *Energy Fuels* **1987**, *1*, 36.
(3) (a) Silbernagel, B. G.; Mohan, R. R.; Singhal, G. H. *ACS Symp. Ser.* **1984**, *No. 248*, 91. (b) Silbernagel, B. G. *J. Catal.* **1979**, *56*, 315. (c) Asaoka, S.; Nakata, S.; Takeuchi, C. *ACS Symp. Ser.* **1987**, *No. 344*, 275. (d) Rose-Brussin, M.; Moranta, D. *Appl. Catal.* **1984**, *11*, 85. (e) Mitchell, P. C. H.; Scott, C. E.; Bonnelle, J.-P.; Grimblot, J. G. *J. Chem. Soc., Faraday Trans. 1* **1985**, *81*, 1047.

(4) (a) Money, J. K.; Huffman, J. C.; Christou, G. *Inorg. Chem.* **1985**, *24*, 3297. (b) Money, J. K.; Folting, K.; Huffman, J. C.; Collison, D.; Temperly, J.; Mabbs, F. E.; Christou, G. *Inorg. Chem.* **1986**, *25*, 4583. (c) Money, J. K.; Huffman, J. C.; Christou, G. *J. Am. Chem. Soc.* **1987**, *109*, 2210. (d) Money, J. K.; Folting, K.; Huffman, J. C.; Christou, G. *Inorg. Chem.* **1987**, *26*, 944. (e) Money, J. K.; Huffman, J. C.; Christou, G. *Inorg. Chem.* **1988**, *27*, 507.

The present work originates from our desire to initiate analogous investigations with a monodentate thiolate, suspecting that these would lead to new species with structural, physicochemical, and/or reactivity characteristics distinctly different from those seen to date with edt^{2-}. Initial work has been concentrated at the V^{III}/V^{IV} level. We herein report our first successes in this area, including a most unusual dinuclear V^{III} complex that contains both a metal—metal bond and an antiferromagnetic exchange interaction. Portions of this work have been communicated.[5b]

Experimental Section

All syntheses were carried out under anaerobic conditions using standard Schlenk and glovebox techniques. MeCN was freshly distilled from calcium hydride; THF, diethyl ether, and hexanes were distilled from sodium/benzophenone. VCl₃(THF)₃ was prepared from VCl₃ (Aldrich) as described in the literature.[6] NaSPh was prepared in THF from sodium metal and benzenethiol (Aldrich). Tetraalkylammonium salts (Aldrich, Kodak) were recrystallized before use from EtOH/Et₂O. 2,2′-Bipyridine (Aldrich) was used as received. (NEt₄)[VCl₄(bpy)][7] and [V(SPh)₂(bpy)₂](PF₆)[8] were prepared as described elsewhere.

(NEt₄)[V(SPh)₄(bpy)] (1). *Method A.* VCl₃(THF)₃ (0.747 g, 2.00 mmol), NaSPh (1.32 g, 10.0 mmol), and NEt₄Cl (0.331 g, 2.00 mmol) were placed in a 100 mL Schlenk flask in a glovebox. The flask was brought into the laboratory, MeCN (40 mL) added by syringe, and the mixture stirred for 30 min. Solid bpy (0.308 g, 2.00 mmol) was then added, causing the orange slurry to dissolve and produce a deep red-purple solution. The solution was stirred for a further 4—5 h and filtered. The filtrate produced a black microcrystalline solid on overnight storage at room temperature. The yield was 34%. Larger crystals can be obtained by heating the filtrate to 60 °C, removing 5—10 mL of solvent under vacuum, and allowing the solution to cool slowly to room temperature. Anal. Calcd (found) for C₄₂H₄₈N₃S₄V: C, 65.17 (64.70); H, 6.25 (6.31); N, 5.43 (5.53); V, 6.58 (6.32). Electronic spectrum in MeCN [λ_{max}/nm (ϵ_M/L mol^{-1} cm^{-1})]: 510 (2600); 550 (sh). Solid-state effective magnetic moment: μ_{eff} = 2.7 μ_B (∼25 °C).

Method B. (NEt₄)[VCl₄(bpy)] (1.0 g, 2.0 mmol) and NaSPh (1.32 g, 10.0 mmol) were dissolved with stirring in MeCN (35 mL) to give a red-purple solution and an off-white solid (NaCl). After 4 h, the latter was removed by filtration and the filtrate stored at room temperature overnight. The resultant microcrystalline solid was collected by filtration, washed with Et₂O (10 mL), and dried *in vacuo*. The yield was ∼50%. The identity of the product was confirmed by spectroscopic comparisons with material from method A.

(NMe₄)[VO(SPh)₃(Me₂-bpy)] (2). VCl₃(THF)₃ (0.747 g, 2.00 mmol), NaSPh (1.32 g, 10.0 mmol), and NMe₄Cl (0.219 g, 2.00 mmol) were placed in a 100 mL Schlenk flask and brought into the laboratory, and MeCN (40 mL) was added by syringe. The resultant orange slurry was stirred for 1 h, and Me₂-bpy (0.368 g, 2.00 mmol) was added to give a red-purple solution. The solution was filtered and air (125 mL, 1.11 mmol O₂) bubbled in portions by syringe into the filtrate over 2—3 h. During this process, the solution slowly turned deep orange-brown. The solution was then deaerated and stored overnight at room temperature. The resultant dark brown solid was collected by filtration, washed with Et₂O, and dried *in vacuo*. The yield was ∼70%. Crystals suitable for crystallography were obtained from an MeCN/Et₂O/hexanes layering. The NEt₄⁺ salt and the bpy analogue of **2** can be prepared in a similar fashion. Anal. Calcd (found) for C₃₄H₃₉N₃OS₃V: C, 62.55 (62.96); H, 6.02 (5.54); N, 6.44 (6.55). Electronic spectrum in MeCN: 472 (770), 708 (140). IR spectrum (NEt₄⁺ salt): 937 cm^{-1}

(5) (a) Heinrich, D. D.; Folting, K.; Huffman, J. C.; Reynolds, J. G.; Christou, G. *Inorg. Chem.* **1991**, *30*, 300. (b) Dean, N. S.; Folting, K.; Lobkovsky, E.; Christou, G. *Angew. Chem., Int. Ed. Engl.* **1993**, *32*, 594. (c) York, K. A.; Folting, K.; Christou, G. *J. Chem. Soc., Chem. Commun.* **1993**, 1563.

(6) Manzer, L. E. *Inorg. Synth.* **1983**, *21*, 135.

(7) (a) Fowles, G. W. A.; Green, P. T. *J. Chem. Soc. A* **1967**, 1869. (b) Clark, R. J. H.; Nyholm, R. S.; Scaife, D. E. *J. Chem. Soc. A* **1966**, 1296. (c) Clark, R. J. H.; Casey, A. T. *Trans. Met. Chem.* **1977**, *2*, 76.

(8) Dean, N. S.; Christou, G. Results to be published.

Table 1. Crystallographic Data for Complexes **2** and **4**

	2	**4·THF**
formula	C₃₄H₃₉N₃OS₃V	C₅₂H₅₂N₄O₂S₄V₂^a
fw	652.82	995.13
space group	*C2/c*	*C2/c*
a, Å	28.618(5)	16.954(3)
b, Å	10.053(1)	15.969(2)
c, Å	24.194(3)	18.830(3)
β, deg	113.40(1)	107.96(1)
V, Å^3	6387.8	4849.5
Z	8	4
T, °C	−157	−173
radiation, Å^b	0.71069	0.71069
ϱ_{calc}, g/cm^3	1.36	1.36
μ, cm^{-1}	5.191	5.808
R_{merge}	0.031	0.075
R (R_w)^{c,d}	0.0585 (0.0581)	0.0644 (0.0646)

^{a} Including solvate molecules. ^{b} Graphite monochromator. ^{c} $R = \Sigma||F_o| - |F_c||/\Sigma|F_o|$. ^{d} $R_w = [\Sigma w(|F_o| - |F_c|)^2/\Sigma w|F_o|^2]^{1/2}$, where $w = 1/\sigma^2(|F_o|)$.

(VO stretch). EPR spectra in MeCN: fluid solution at 298 K; g_{iso} = 1.973, A_{iso} = 86.4 G, frozen glass at 100 K, $g_{\parallel}$ = 1.962, $A_{\parallel}$ = 162.2 G, $g_\perp$ = 1.978, $A_\perp$ = 48.6 G.

[VO(SPh)(bpy)₂](PF₆) (3). Air (65 mL, ∼0.6 mmol O₂) was slowly bubbled by syringe over the course of 3 h through a solution of [V(SPh)₂(bpy)₂](PF₆) (0.72 g, 1.0 mmol); the solution color slowly changed from dark red to dark orange/brown. The flask was then deaerated and the solvent removed under vacuum to give a dark brown solid. This was slurried with Et₂O, collected by filtration, washed with Et₂O, and dried *in vacuo*. The yield was ∼75%. Anal. Calcd (found) for C₂₈H₂₆N₄O₁.₅F₆PSV (**3**·¹/₂Et₂O): C, 50.16 (50.88); H, 3.91 (3.61); N, 8.36 (8.57). Electronic spectrum in MeCN: 472 (773), 704 (140). IR spectrum: 970 cm^{-1}. EPR spectrum in MeCN (298 K): g_{iso} = 1.978, A_{iso} = 89 G.

V₂O(SPh)₄(Me₂-bpy)₂ (4). *Method A.* VCl₃(THF)₃ (0.747 g, 2.00 mmol), NaSPh (0.798 g, 6.00 mmol), and Me₂-bpy (0.368 g, 2.00 mmol) were dissolved in MeCN (40 mL). After 2 h the solution was filtered to remove NaCl, and water (18 μL, 1.0 mmol) was added to the filtrate by syringe. The solution slowly changed color from red-purple to purple. The flask was left undisturbed for 2 days at room temperature, during which time dark green crystals formed. These were collected by filtration, washed with CH₃CN, and dried *in vacuo*. The yield was 20—25%. Elemental analysis indicated the formulation **4**·¹/₂MeCN. Anal. Calcd (found) for C₄₉H₄₅.₅N₄.₅OS₄V₂: C, 62.37 (62.04); H, 4.86 (4.83); N, 6.68 (6.45); S, 13.59 (13.52); V, 10.80 (9.98). Electronic spectrum in THF: 400 (2160), 584 (814). Crystals of **4**·THF suitable for crystallography were obtained by recrystallization from a THF solution stored at −20 °C.

Method B. This procedure uses THF as the reaction medium. VCl₃-(THF)₃ (0.747 g, 2.00 mmol), NaSPh (0.798 g, 6.00 mmol), and Me₂-bpy (0.368 g, 2.00 mmol) were dissolved with stirring in THF (40 mL). After 1 h, water (18 μL, 1.0 mmol) was added and the solution color changed rapidly from red-purple to dark green. After a further 1 h, the solution was filtered and the filtrate volume reduced to ∼10 mL. Ether (40 mL) was added, and a dark green powder of **4** was precipitated. This was collected by filtration, washed with Et₂O, and dried *in vacuo*. The yield was 40—45%. The spectroscopic properties of this product were identical to those of material obtained from the reaction in MeCN.

X-ray Crystallography and Structure Solution. Data were collected for complexes **2** and **4** on a Picker four-circle diffractometer; details of the diffractometry, low-temperature facilities, and computational procedures employed by the Molecular Structure Center are available elsewhere.[9] Suitable crystals were chosen from samples examined inside a nitrogen glovebag, attached to glass fibers using silicone grease and then transferred quickly to the goniostat where they were cooled in a nitrogen gas cold-stream for characterization and data collection. Data collection parameters are summarized in Table 1. For

(9) Chisholm, M. H.; Folting, K.; Huffman, J. C.; Kirkpatrick, C. C. *Inorg. Chem.* **1984**, *23*, 1021.

both complexes, the structures were solved by the usual combination of direct methods (MULTAN) and Fourier techniques and refined by full-matrix least-squares cycles.

For complex **2**, a systematic search of a limited hemisphere of reciprocal space revealed intensities with $2/m$ Laue symmetry and the general condition $h + k = 2n$ for hkl. Following the complete intensity data collection for the C-centered monoclinic cell, the additional condition $h = 2n$ and $l = 2n$ for $h0l$ limited the space group to $C2/c$ or Cc. Space group $C2/c$ was selected initially, and it was confirmed by the successful solution of the structure. Four standards measured every 400 data showed no systematic trends. No correction was made for absorption. Most of the structure was revealed in the initial MULTAN E-map. The remainder of the atoms, including most of the hydrogens, were found in subsequent iterations of least-squares refinement cycles and difference Fourier map calculations. The remaining hydrogen atoms were initially placed in calculated positions and their positions then refined. In the final cycles of least-squares refinement, the non-hydrogen atoms were varied with anisotropic thermal parameters and the hydrogen atoms were varied with isotropic thermal parameters. The final difference map was featureless, the largest peak being 0.45 e/Å^3. Final values of R (R_w) are listed in Table 1.

For complex **4**, a systematic search of a limited hemisphere of reciprocal space also revealed symmetry and systematic absences corresponding to the two monoclinic space groups $C2/c$ and Cc. An initial choice of centrosymmetric $C2/c$ was confirmed by the successful solution of the structure. Intensity data were weak, with only 50% being "observed" on the criteria $F > 3\sigma(F)$. No correction was made for absorption. The V and S atom positions were obtained from an initial E-map, and the remainder of the non-hydrogen atoms were found in subsequent iterations of least-squares refinement cycles and difference Fourier map calculations. After partial refinement of the non-hydrogen atoms, hydrogen atoms were included in fixed calculated positions. In the final refinement cycles, all non-hydrogen and hydrogen atoms were refined with anisotropic and isotropic thermal parameters, respectively. The V-containing molecule lies on a crystallographic 2-fold rotation axis passing through bridging oxygen atom O(4). The THF molecule is also on a 2-fold axis necessitating a disorder in the oxygen atom O(31) and an occupancy of 0.50. A void of radius 2.6 Å was located with its center at position $x = 0.438$, $y = 0.158$, $z = 0.136$. The largest peak in the final difference Fourier map (1.04 e/Å^3) is located in this void, suggesting a badly disordered solvent molecule may possibly be lying at this position. Final values of R (R_w) are listed in Table 1.
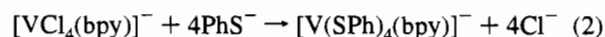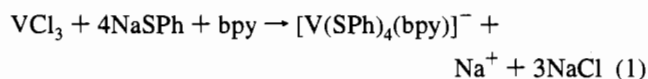
Physical Measurements. NMR spectra were recorded on a Varian XL300 spectrometer. IR spectra were taken on Nujol mulls between CsI plates using a Nicolet 510P FTIR spectrophotometer. Electronic spectra were recorded with a Hewlet-Packard 8452A diode array spectrophotometer in the range 190−820 nm. Room-temperature magnetic measurements were made with a Johnson-Matthey magnetic susceptibility balance. Variable-temperature magnetic measurements were made with a Quantum Design MPMS SQUID susceptometer operating with a 10 kG (1 T) applied magnetic field. Problems were encountered with liquid oxygen condensation on the sample leading to significant spikes in the χ_M vs T data in the 30−90 K region. These were minimized but not totally eliminated by repeatedly sweeping the temperature through this range. EPR spectra were recorded using a Bruker ESP300 spectrometer. Quoted g and A values have been corrected for second-order effects. Elemental analyses were performed by Oneida Research Service or Galbraith Laboratories.

Molecular Orbital Calculations. Calculations were performed on the model complex $V_2O(SH)_4(NH_3)_4$ using the EHT method with weighted H_{ij}'s; the parameters for V, S, O, N, and H were taken from the literature.[10] Atomic coordinates for the V, S, O, and N atoms were taken from the crystallographic data for **4**.

Results

Syntheses. The thiol chosen for the present studies is benzenethiol, which we have not employed previously in V^{III} chemistry; a bulkier version, 2,6-diisopropylbenzenethiolate (dipt) has been used by others in the preparation of the V^{III} complex V(dipt)$_3$(THF)$_2$.[11] In contrast to dipt, whose bulky Pr^i groups prevent polymer formation with V^{III} reagents, the addition of NaSPh to solutions of VCl$_3$ or VCl$_3$(THF)$_3$, in a V:SPh ratio of 1:4 or higher, leads to formation of an insoluble dark orange solid, presumably the thiolate-bridged polymer [V(SPh)$_3$]$_n$. In previous work, we had shown that reaction of such V^{III}/PhS$^-$ slurries with elemental sulfur leads to metal oxidation and the formation of [VS(SPh)$_4$]$^{2-}$ or [VS$_2$(S$_2$)(SPh)]$^{2-}$ salts, depending on the V:S ratio.[12] In the present work, however, we desired to obtain soluble V^{III}/SPh products, and it was therefore decided to attempt to overcome polymer formation by addition of a chelate that might foster formation of discrete products; the chelates chosen were 2,2'-bipyridine (bpy) and its 4,4'-dimethyl analogue (Me$_2$-bpy).

Addition of 1 equiv of bpy to the orange slurry obtained from VCl$_3$(THF)$_3$/NaSPh/NEt$_4$Cl in a 1:5:1 ratio in MeCN leads to rapid dissolution of the solid and the formation of a deep red-purple solution from which was isolated black microcrystals of (NEt$_4$)[V(SPh)$_4$(bpy)] (**1**) after unexceptional workup. Larger crystals were found to diffract well, but a large unit cell (c axis ∼38 Å) dissuaded us from pursuing a structure solution; there is little doubt as to the formulation of this molecule as a six-coordinate, distorted-octahedral mononuclear complex. The formation of the anion of **1** is summarized in eq 1. An

$$VCl_3 + 4NaSPh + bpy \rightarrow [V(SPh)_4(bpy)]^- +$$
$$Na^+ + 3NaCl \quad (1)$$

$$[VCl_4(bpy)]^- + 4PhS^- \rightarrow [V(SPh)_4(bpy)]^- + 4Cl^- \quad (2)$$

alternative route to **1** is available via the known complex (NEt$_4$)-[VCl$_4$(bpy)],[7] as summarized in eq 2. Both of the described procedures are extremely convenient and provide ready access to adequate yields of **1** for further investigations.

The main objective in reactivity studies on **1** has been incorporation of oxygen to give oxide-containing products at the V^{III} and V^{IV} levels. Two procedures have proven useful, controlled oxidation with O$_2$ and controlled hydrolysis. Slow bubbling of air through a red-purple solution of [V(SPh)$_4$(Me$_2$-bpy)]$^-$, generated *in situ* in a manner analogous to that for **1**, causes a color change to deep orange-brown and subsequent isolation in 70% yield of (NMe$_4$)[VO(SPh)$_3$(Me$_2$-bpy)] (**2**) (or the corresponding NEt$_4^+$ salt). The presence of a strong band in the 900−1000 cm^{-1} region of the IR spectrum characteristic of the VO triple bond stretch was the first indication that a [VO]$^{2+}$ complex had been obtained; this was subsequently confirmed by the elemental analysis, the EPR spectrum, and, ultimately, the crystallographic data (*vide infra*). The formation of **2** from **1** is summarized in eq 3, assuming that the second

$$[V(SPh)_4(bpy)]^- + {}^1/_2O_2 \rightarrow [VO(SPh)_3(bpy)]^- + {}^1/_2PhSSPh \quad (3)$$
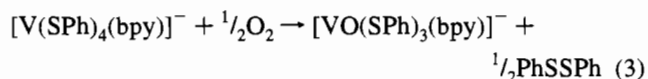
(10) (a) Ammeter, J. H.; Burgi, H.-B.; Thibeault, J. C.; Hoffmann, R. *J. Am. Chem. Soc.* **1978**, *100*, 3686. (b) Kubácek, P.; Hoffmann, R.; Haulas, Z. *Organometallics* **1982**, *1*, 180. (c) Chen, M. M. L.; Hoffmann, R. *J. Am. Chem. Soc.* **1976**, *98*, 1647. (d) Hoffmann, R. *J. Chem. Phys.* **1963**, *39*, 1397.

(11) Randall, C. R.; Armstrong, W. H. *J. Chem. Soc., Chem. Commun.* **1988**, 986.

(12) (a) Money, J. K.; Nicholson, J. R.; Huffman, J. C.; Christou, G. *Inorg. Chem.* **1986**, *25*, 4072. (b) Nicholson, J. R.; Huffman, J. C.; Ho, D.; Christou, G. *Inorg. Chem.* **1987**, *26*, 3030.
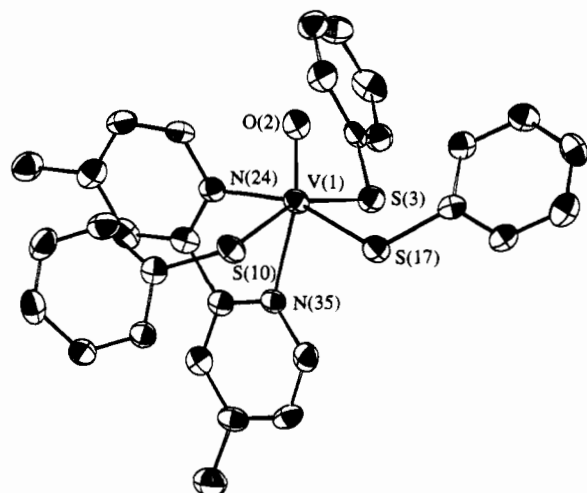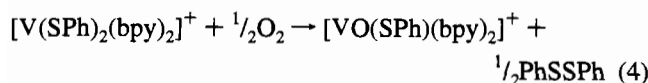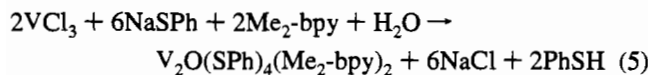
Figure 1. ORTEP representation of the anion of complex **2** depicted at the 50% probability level. Carbon atoms are numbered sequentially around aromatic rings.

$$[V(SPh)_2(bpy)_2]^+ + {}^1/_2O_2 \rightarrow [VO(SPh)(bpy)_2]^+ + {}^1/_2PhSSPh \quad (4)$$

oxidizing equivalent generates PhSSPh. The same reaction but with $[V(SPh)_2(bpy)_2](PF_6)$ was found to lead to the corresponding $[VO]^{2+}$ complex $[VO(SPh)(bpy)_2](PF_6)$ (**3**), the formation of which is summarized in eq 4. Complex **3** has not been structurally characterized, but its elemental analysis and IR and EPR spectra are sufficient for identification purposes.

Hydrolysis of the Me₂-bpy version of **1** or, more conveniently, a VCl₃/NaSPh/Me₂-bpy (1:3:1) reaction mixture with 0.5 equiv of water provides a convenient route to the dark green dinuclear V^{III} product $V_2O(SPh)_4(Me_2\text{-}bpy)_2$ (**4**). Yields of **4** are significantly higher in a THF rather than MeCN reaction medium, but both solvents provide product in high purity and crystallinity. The formation of **4** is summarized in eq 5, assuming liberated PhS⁻ acts as the proton acceptor. In both the aerial oxidation and hydrolysis reactions of eqs 3–5, the PhS⁻ groups presumably assist clean reaction by functioning as electron donors and proton acceptors, as indicated in the balanced equations.

$$2VCl_3 + 6NaSPh + 2Me_2\text{-}bpy + H_2O \rightarrow$$
$$V_2O(SPh)_4(Me_2\text{-}bpy)_2 + 6NaCl + 2PhSH \quad (5)$$

Description of Structures. ORTEP representations of the anion of **2** and complex **4** are shown in Figures 1 and 2, respectively; fractional coordinates and bond distances and angles for **2** and **4** are listed in Tables 2 and 4 and Tables 3 and 5, respectively.

The anion of **2** consists of a six-coordinate V^{IV} atom ligated by three PhS⁻ and one Me₂-bpy groups, in addition to the triply-bonded oxygen atom. The metal geometry is severely distorted octahedral, with the strong *trans*-influence of the multiply-bonded O atom leading to a significant lengthening of the axial V(1)–N(35) bond (2.331(4) Å) compared with the equatorial V(1)–N(24) bond (2.155(4) Å). The V–O distance (1.612(4) Å) is reasonable given the *trans* N ligand, although an even larger value has been seen for *five*-coordinate $[VO(edt)_2]^{2-}$ (1.625(2) Å); the latter has been assigned to the good π-donor properties of four alkanethiolate S atoms and the overall negative charge.[4a] It is interesting to note in **2** that the *trans* V(1)–S(3) and V(1)–S(10) bonds (2.464(2) and 2.450(2) Å) are noticeably longer than the V(1)–S(17) bond (2.402(2) Å), which is *trans* to a bpy N atom, consistent with a significant difference in the
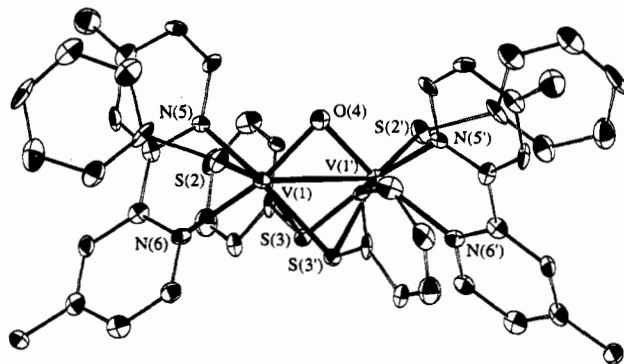

Figure 2. ORTEP representation of complex **4** depicted at the 50% probability level. Carbon atoms are numbered sequentially around aromatic rings.

Table 2. Fractional Coordinates ($\times 10^4$) and Equivalent Isotropic Thermal Parameters ($Å^2 \times 10$) for $(NMe_4)[VO(SPh)_3(Me_2\text{-}bpy)]$ (**2**)

atom	x	y	z	$B_{eq}{}^a$
V(1)	1725.3(3)	1565(1)	1008.8(4)	21
O(2)	1851(1)	2716(4)	625(2)	25
S(3)	1736(1)	−415(1)	413(1)	24
C(4)	1393(2)	−185(6)	−369(2)	22
C(5)	1229(2)	−1278(6)	−747(3)	27
C(6)	980(2)	−1138(6)	−1358(3)	32
C(7)	880(2)	108(7)	−1614(3)	31
C(8)	1047(2)	1206(6)	−1252(3)	32
C(9)	1300(2)	1064(6)	−638(3)	29
S(10)	1733(1)	2836(2)	1876(1)	26
C(11)	1099(2)	3024(5)	1818(2)	22
C(12)	900(2)	2121(6)	2109(2)	25
C(13)	401(2)	2245(6)	2060(3)	28
C(14)	106(2)	3285(7)	1741(3)	32
C(15)	300(2)	4190(6)	1463(3)	32
C(16)	792(3)	4057(6)	1497(3)	31
S(17)	2543(1)	1021(2)	1777(1)	25
C(18)	3022(2)	684(5)	1505(2)	20
C(19)	3476(2)	155(6)	1908(2)	24
C(20)	3877(2)	−132(6)	1747(3)	31
C(21)	3817(2)	109(6)	1162(3)	30
C(22)	3370(2)	636(6)	751(2)	27
C(23)	2971(2)	933(6)	915(2)	24
N(24)	916(2)	1860(4)	542(2)	21
C(25)	736(2)	2871(6)	149(2)	25
C(26)	234(2)	3230(6)	−110(2)	27
C(27)	−125(2)	2533(6)	25(2)	28
C(28)	57(2)	1471(6)	425(3)	27
C(29)	573(2)	1155(5)	677(2)	23
C(30)	789(2)	88(5)	1127(2)	21
C(31)	496(2)	−737(6)	1324(2)	24
C(32)	728(2)	−1662(6)	1772(2)	25
C(33)	1257(2)	−1738(6)	2004(2)	25
C(34)	1523(2)	−889(6)	1782(2)	26
N(35)	1299(2)	18(4)	1357(2)	21
C(36)	−671(2)	2911(6)	−230(3)	32
C(37)	421(3)	−2506(6)	2007(3)	35

$^a B_{eq} = {}^4/_3 \sum\sum B_{ij}a_ia_j.$

trans influence of PhS⁻ S atoms *vs* bpy N atoms. The phenyl ring attached to S(10) is lying over and essentially parallel with the bpy plane, an arrangement clearly due to π-stacking interactions.

The structure of **4**·THF consists of well-separated [V₂O(SPh)₄-(Me₂-bpy)₂] and THF molecules that are both lying on crystallographic 2-fold axes. The V₂O molecule contains two V^{III} atoms triply-bridged by the O^{2-} and two PhS⁻ groups. The 2-fold axis passes through O(4) and the midpoint of the S(3)·‑S-(3′) vector. Terminal ligation at each V is provided by a PhS⁻ and a chelating Me₂-bpy group. The metals are thus six-coordinate with severely distorted octahedral geometry, due in part to the restricted bite angle of the Me₂-bpy groups. The

Table 3. Fractional Coordinates ($\times 10^4$)^a and Equivalent Isotropic Thermal Parameters ($\text{Å}^2 \times 10$) for $[V_2O(SPh)_4(Me_2\text{-bpy})_2]\cdot THF$ (**4**)

atom	x	y	z	$B_{eq}{}^a$
V(1)	294(1)	1633(1)	6944(1)	11
S(2)	−378(1)	2087(1)	5692(1)	16
S(3)	−837(1)	699(1)	6952(1)	11
O(4)	0*	2455(5)	7500*	14
N(5)	1447(4)	2279(4)	7090(3)	10
N(6)	1041(4)	829(4)	6465(4)	12
C(7)	411(5)	2404(5)	5306(4)	15
C(8)	651(5)	1880(6)	4823(5)	21
C(9)	1239(6)	2109(7)	4485(5)	29
C(10)	1577(6)	2890(6)	4625(6)	30
C(11)	1355(6)	3438(6)	5097(5)	28
C(12)	781(5)	3193(6)	5434(5)	24
C(13)	−1893(4)	998(5)	6481(4)	12
C(14)	−2123(5)	1784(5)	6184(4)	11
C(15)	−2955(5)	1962(6)	5834(4)	18
C(16)	−3544(5)	1358(6)	5794(5)	20
C(17)	−3313(5)	568(6)	6098(5)	23
C(18)	−2483(5)	380(5)	6440(4)	15
C(19)	1596(5)	3053(5)	7387(4)	15
C(20)	2348(5)	3431(5)	7550(4)	13
C(21)	3030(5)	3008(5)	7449(4)	17
C(22)	2855(5)	2206(5)	7134(4)	16
C(23)	2067(5)	1866(5)	6944(4)	13
C(24)	1836(5)	1063(5)	6570(4)	13
C(25)	2373(5)	573(5)	6310(4)	15
C(26)	2093(5)	−144(5)	5893(4)	16
C(27)	1259(5)	−353(5)	5765(4)	17
C(28)	768(5)	137(5)	6069(4)	15
C(29)	3885(6)	3354(6)	7665(5)	26
C(30)	2644(6)	−660(5)	5591(5)	20

^{a} Parameters marked with an asterisk were fixed by symmetry. ^{b} B_{eq} = $^4/_3$ $\sum\sum B_{ij}a_ia_j$.

Table 4. Selected Distances and Angles for $(NMe_4)[VO(SPh)_3(Me_2\text{-bpy})]$ (**2**)

(a) Bonds (Å)			
V(1)−S(3)	2.4643(17)	V(1)−O(2)	1.612(4)
V(1)−S(10)	2.4503(17)	V(1)−N(24)	2.155(4)
V(1)−S(17)	2.4018(16)	V(1)−N(35)	2.331(4)

(b) Angles (deg)			
S(3)−V(1)−S(10)	157.55(6)	S(17)−V(1)−O(2)	103.73(13)
S(3)−V(1)−S(17)	91.95(6)	S(17)−V(1)−N(24)	161.77(12)
S(3)−V(1)−O(2)	100.70(14)	S(17)−V(1)−N(35)	93.30(11)
S(3)−V(1)−N(24)	93.74(12)	O(2)−V(1)−N(24)	92.21(17)
S(3)−V(1)−N(35)	78.62(11)	O(2)−V(1)−N(35)	162.97(17)
S(10)−V(1)−S(17)	77.38(5)	N(24)−V(1)−N(35)	70.94(16)
S(10)−V(1)−O(2)	101.00(14)	V(1)−S(3)−C(4)	112.95(19)
S(10)−V(1)−N(24)	91.10(12)	V(1)−S(10)−C(11)	109.04(17)
S(10)−V(1)−N(35)	82.30(11)	V(1)−S(17)−C(18)	114.55(18)

complex has imposed C_2 symmetry. The central $[V_2(\mu\text{-O})(\mu\text{-}SPh)_2]^{2+}$ unit is unique for vanadium and extremely rare for any metal; it has been found previously only in a highly unsymmetrical form in dinuclear Mo complexes. In these examples, there is an almost planar Mo_2OS unit involving one of the two RS^- sulfur atoms, and the other RS^- forms longer, weaker Mo−S bonds.[13] The $[M_2(\mu\text{-OH})(\mu\text{-SPh})_2]$ core is known, for example in the complex $[Cp_2Mo_2(OH)(SPh)_2Cl_2]$,[14] and some examples of species with $[M_2(\mu\text{-S})(\mu\text{-SR})_2]$ cores are also known.[15]

(13) (a) Dilworth, J. R.; Neaves, B. D.; Dahlstrom, P.; Hyde, J.; Zubieta, J. A. *Trans. Met. Chem.* **1982**, *7*, 257. (b) Yamanouchi, K.; Enemark, J. E.; McDonald, J. W.; Newton, W. E. *J. Am. Chem. Soc.* **1977**, *99*, 3529.

(14) Couldwell, C.; Meunier, B.; Prout, K. *Acta Crystallogr., Sect. B* **1979**, *B35*, 603.

(15) (a) Boorman, P. M.; Kerr, K. A.; Patel, V. D. *J. Chem. Soc., Dalton Trans* **1981**, 506. (b) Wolf, T. E.; Berg, J. M.; Hodgson, K. O.; Frankel, R. B.; Holm, R. H. *J. Am. Chem. Soc.* **1979**, *101*, 4140.

Table 5. Selected Distances and Angles for $[V_2O(SPh)_4(Me_2\text{-bpy})_2]\cdot THF$ (**4**)

(a) Bonds (Å)			
V(1)−V(1)	2.579(3)	V(1)−O(4)	1.841(6)
V(1)−S(2)	2.394(3)	V(1)−N(5)	2.152(6)
V(1)−S(3)	2.432(2)	V(1)−N(6)	2.184(7)

(b) Angles (deg)			
V(1′)−V(1)−S(2)	127.89(9)	S(3′)−V(1)−O(4)	92.76(15)
V(1′)−V(1)−S(3)	59.56(6)	S(3′)−V(1)−N(5)	95.34(17)
V(1′)−V(1′)−S(3)	57.28(6)	S(3)−V(1)−N(5)	168.52(18)
V(1′)−V(1)−O(4)	45.53(17)	S(3)−V(1)−N(6)	101.58(18)
V(1′)−V(1)−N(5)	117.37(17)	S(3′)−V(1)−N(6)	83.15(18)
V(1′)−V(1)−N(6)	138.87(17)	O(4)−V(1)−N(5)	88.86(20)
S(2)−V(1)−S(3′)	160.79(9)	O(4)−V(1)−N(6)	161.25(19)
S(2)−V(1)−S(3)	93.16(8)	N(5)−V(1)−N(6)	73.39(23)
S(2)−V(1)−O(4)	102.36(14)	V(1)−S(2)−C(7)	107.43(25)
S(2)−V(1)−N(5)	96.72(17)	V(1)−S(3)−V(1′)	63.15(8)
S(2)−V(1)−N(6)	86.03(18)	V(1′)−S(3)−C(13)	107.94(27)
S(3)−V(1)−S(3′)	73.63(9)	V(1)−S(3)−C(13)	120.04(27)
S(3)−V(1)−O(4)	94.74(15)	V(1)−O(4)−V(1′)	88.9(3)

Table 6. Structurally-Characterized Examples of $[V-O-V]^{4+}$ Complexes

complex^a	V−O−V type	V··V, Å	V−O−V, deg	V−O, Å	ref
4	bent	2.579(3)	88.9(3)	1.841(6)	b
$[V_2O(OAc)_2(tacn)_2]^{2+}$	bent	3.250(2)	130.2(2)	1.792[3]^c	16
$V_2O(OAc)_2(HB(pz)_3)_2$	bent	3.264(n)	133.3(n)	1.777(n)	17
$V_2OCl_4(THF)_6$	linear	d	180	1.769(5)	18
$V_2OCl_4(py)_6$	linear	d	179.1(5)	1.775(6)	19
$V_2O(Me_2\text{-aet})_4$	linear	d	177.84(25)	1.813[10]^c	4d
$[V_2OCl_2(bpy)_4]^{2+}$	linear	d	173.5(3)	1.787(1)	20
$[V_2O(acac)_2(tacn)_2]^{2+}$	linear	d	180	1.806(1)	21
$V_2O(BH_4)_4(PMe_3)_4$	linear	d	178.7(1)	1.781[2]^c	22
$V_2O(SPh)_2(bpy)_4$	linear	d	167.7(4)	1.800(1)	8

^{a} tacn = 1,4,7-trimethyl-1,4,7-triazacyclononane; HB(pz)$_3$ = hydridotris(2-pyrazolyl)borate; Me$_2$-aet = 2-(dimethylamino)ethanethiolate; acac = acetylacetonate. ^{b} This work. ^{c} Average of two values; the number in brackets is the variation about the average. ^{d} >3.4 Å. n = not reported.

Dinuclear V^{III} complexes with a bridging oxide are now fairly common, but most of these contain a linear $[V-O-V]^{4+}$ unit, rather than a bent one as in **4**. Previous examples are collected in Table 6, where it can be seen that only two other examples of a bent $[V-O-V]^{4+}$ unit have been reported. Although the first three entries all possess three bridging ligands, **4** is the only one to have three *mono*atomic bridges (the AcO$^-$ groups bridging in their familiar bidentate $\eta^1:\eta^1$ mode with a *syn,syn* conformation) and a V··V separation suggestive of metal−metal bonding (*vide infra*). As a result, the V−O−V angle (88.9-(3)°) is much more acute and the V−O distance (1.841(6) Å) is slightly greater than for the other complexes, the latter probably as a result of decreased V−O π interactions and less s-character in the V−O bonds at a V−O−V angle of ∼90°.

The V··V separation of 2.579(3) Å is indicative of a metal−metal bonding interaction; a distance of ∼2.6 Å is characteristic of a $V^{III}-V^{III}$ single bond. Complex **4** represents the third such example containing bridging S ligands, the others being

(16) Koppen, M.; Fresen, G.; Wieghardt, K.; Llusar, R. M.; Nuber, B.; Weiss, J. *Inorg. Chem.* **1988**, *27*, 721.

(17) Carrano, C. J.; Verastgue, R.; Bond, M. R. *Inorg. Chem.* **1993**, *32*, 3589.

(18) Chandrasekhar, P.; Bird, P. H. *Inorg. Chem.* **1984**, *23*, 3677.

(19) Rambo, J. R.; Christou, G. Results to be published.

(20) Brand, S. G.; Edelstein, N.; Hawkins, C. J.; Shalimoff, G.; Snow, M. R.; Tiekink, E. R. T. *Inorg. Chem.* **1990**, *29*, 434.

(21) Knopp, P.; Wieghardt, K.; Nuber, B.; Weiss, J.; Sheldrick, W. S. *Inorg. Chem.* **1990**, *29*, 363.

(22) Jensen, J. A.; Girolami, G. *Inorg. Chem.* **1989**, *28*, 2114.

Table 7. Dinuclear Vanadium/Chalcogen Complexes with V–V Single Bonds

compd	ox. state	bridging atoms[a]	V··V, Å	ref
4	III	3	2.579(3)	b
[V$_2$(edt)$_4$]$^{2-}$	III	4	2.600(1)	4e
Cp$_2$V$_2$(edt)$_2$	III	4	2.541(1)	24
Cp′$_2$V$_2$S$_4$	IV	4[c]	2.610(1)	25
Cp$_2$V$_2$S$_2$(S$_2$C$_4$F$_6$)	IV	4	2.574(3)	25
Cp″$_2$V$_2$S$_5$	IV	5[d]	2.658(1)	26
Cp*$_2$V$_2$S$_2$Se$_2$	IV	4[c]	2.641(2)	27
Cp*$_2$V$_2$OSe$_3$	IV	4[c]	2.502(2)	27
[V$_2$(S$_2$)$_2$(CS$_3$)$_4$]$^{4-}$	IV	4	2.872(1)	28
V$_2$(S$_2$)$_2$(S$_2$CMe)$_4$	IV	4	2.800(1)	29
V$_2$(S$_2$)$_2$(S$_2$CNEt$_2$)$_4$	IV	4	2.900(6)	30
V$_2$(S$_2$)$_2$(S$_2$CNBu$_2$)$_4$	IV	4	2.851(2)	31

[a] All are monoatomic-bridging, unless otherwise indicated. [b] This work. [c] Two monoatomic bridges. [d] Three monoatomic bridges.

[V$_2$(edt)$_4$]$^{2-}$ salts[4e,23] and Cp$_2$V$_2$(edt)$_2$.[24] These and a selection of analogous dinuclear V^{IV} complexes with V–V single bonds are listed in Table 7. As can be seen, there are two distinct types: complexes with V··V separations of 2.50–2.66 Å encompassing both V^{III} and V^{IV}; complexes with the quadruply-bridged [V$_2$(μ-S$_2$)$_2$]$^{4+}$ core with V··V separations of 2.8–2.9 Å. The presence of bridging atoms does, of course, complicate a simple metal–metal bonding picture, and there is no doubt that the bridges are involved in the interactions between d electrons on the two sides of the molecules. Nevertheless, it appears that a V–V bonding description is valid and is supported by acute V–S–V angles, which for **4**, for example, are 63.15(8)°.

If a V–V single bond (albeit with bridging S involvement) is entertained for **4** and the other two V^{III}$_2$ complexes, as proposed here and by the previous authors, then the presence of a *single* bond for a d^2–d^2 dimer suggests that the complexes might exhibit paramagnetism from the d electrons not involved in metal–metal bonding. Indeed, **4**, [V$_2$(edt)$_4$]$^{2-}$ and Cp$_2$V$_2$-(edt)$_2$ are all weakly paramagnetic in the solid state at room temperature. However, the μ_{eff} values for the three V^{III}$_2$ complexes (0.96–1.10 μ_B/V) are less than expected for one unpaired electron on each metal (spin-only value of 1.73 μ_B/V). Holm and co-workers have determined from EHT calculations that [V$_2$(edt)$_4$]$^{2-}$ contains a V–V single (σ) bond and a δ/δ* combination of MO's formed from two V d$_{x^2-y^2}$ atomic orbitals; they further suggest that the observed paramagnetism might be due to a thermally-populated triplet excited state resulting from excitation of an electron from the HOMO (δ*) into the nearby (0.17 eV) LUMO (δ).[23a] Such a situation might also be present in **4** (and Cp$_2$V$_2$(edt)$_2$), and it is thus clear that detailed studies on a representative system are warranted. Note that the triply-bridged, face-sharing bioctahedral nature of **4** is distinctly different from the quadruply-bridged dinuclear nature of [V$_2$(edt)$_4$]$^{2-}$ and Cp$_2$V$_2$(edt)$_4$, so that the electronic structure of **4** may or may not be similar to those of the other two complexes. Thus, EHT calculations and variable-temperature magnetochemical studies on **4** have been carried out to probe its electronic structure in detail.

EHT Molecular Orbital Calculation. The objectives were to assess the extent of metal–metal bonding in **4** and to provide a framework and guidance for the interpretation of the VT magnetochemical studies (*vide infra*). The calculation was performed on the model complex V$_2$O(SH)$_4$(NH$_3$)$_4$ of C_2
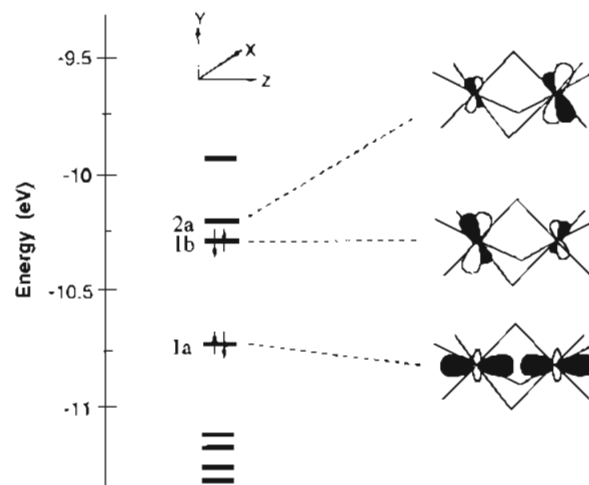

Figure 3. Orbital energy diagram in the HOMO/LUMO region resulting from an EHT MO calculation on the model complex V$_2$O-(SH)$_4$(NH$_3$)$_4$ of C_2 symmetry.

symmetry, and the frontier orbitals pertinent to our objectives are shown in Figure 3. The four lowest-energy orbitals shown are primarily sulfur-based and will not be discussed further. Orbital 1a, the second-highest occupied MO (SHOMO), is composed of a bonding combination of Vd$_{z^2}$ orbitals with ~35% metal character and ~60% bridging-sulfur character; this orbital is interpreted as a V–V single (σ) bond. The Mulliken overlap population is 0.17 electrons, which is similar to that observed[19] for the V–V single bond in [V$_2$(edt)$_4$]$^{2-}$. Orbital 1a lies 0.54 eV (~4400 cm^{-1}) below the HOMO (1b). The latter and the LUMO (2a) approximate δ and δ* orbitals resulting from in-phase and out-of-phase overlap, respectively, of the V d$_{xy}$ orbitals (actually a combination of d$_{xy}$ and d$_{x^2-y^2}$ orbitals on each V). For both 1b and 2a, however, the overlap populations are negligible (<0.04 electrons) and the energy gap between them is extremely small (~0.02 eV, ~150 cm^{-1}), so they can reasonably be described as essentially localized on single metals and, consequently, V–V nonbonding in nature. They have ~80% metal character. The second-lowest unoccupied MO (SLUMO) is 0.31 eV (~2500 cm^{-1}) above the LUMO and is primarily V–S (terminal) π* in character.

The picture that emerges from the EHT calculation is a ground state with a configuration 1a^{2}1b^2 and a net V–V single (σ) bond. The first excited state is a very low-lying triplet state ($S = 1$) of configuration 1a^{2}1b^{1}2a^1 which still retains the V–V single bond. Another triplet state, involving electron excitation into the SLUMO, is at much higher energy (0.31 eV, ~2500 cm^{-1}). The nearest quintet excited state would require electron excitations from the HOMO to the LUMO, and also from the SHOMO to the SLUMO, a total energy of ~0.9 eV (~7300 cm^{-1}).

The results of the EHT calculation on V$_2$O(SH)$_4$(NH$_3$)$_4$ extrapolated to complex **4** suggest the following: (i) It is reasonable to describe complex **4** as containing a V–V single bond. (ii) The paramagnetism observed at room temperature is likely due to thermal population of the triplet (1a^{2}1b^{1}2a^1) excited state. Although EHT calculations do not give accurate values of energies, and are therefore not reliable for predicting the singlet–triplet energy gap in **4**, the calculation does qualitatively suggest that the energy gap is comparable with available thermal energy (~200 cm^{-1} at 300 K). (iii) The V–V bonding orbital (1a) is too low in energy to allow thermal population of a quintet ($S = 2$) state. Thus, complex **4** appears to be electronically similar to [V$_2$(edt)$_4$]$^{2-}$, at least as far as conclusions based on EHT calculations are concerned. Further data are obviously required, but the above picture is fortunately

(23) (a) Pulla Rao, Ch.; Dorfman, J. R.; Holm, R. H. *Inorg. Chem.* **1986**, 25, 428. (b) Szeymies, D.; Krebs, B.; Henkel, G. *Angew. Chem., Int. Ed. Engl.* **1983**, 22, 885.
(24) Rajan, O. A.; McKenna, M.; Noordik, J.; Haltiwanger, R. C.; Rakowski-Dubois, M. *Organometallics* **1984**, 3, 831.
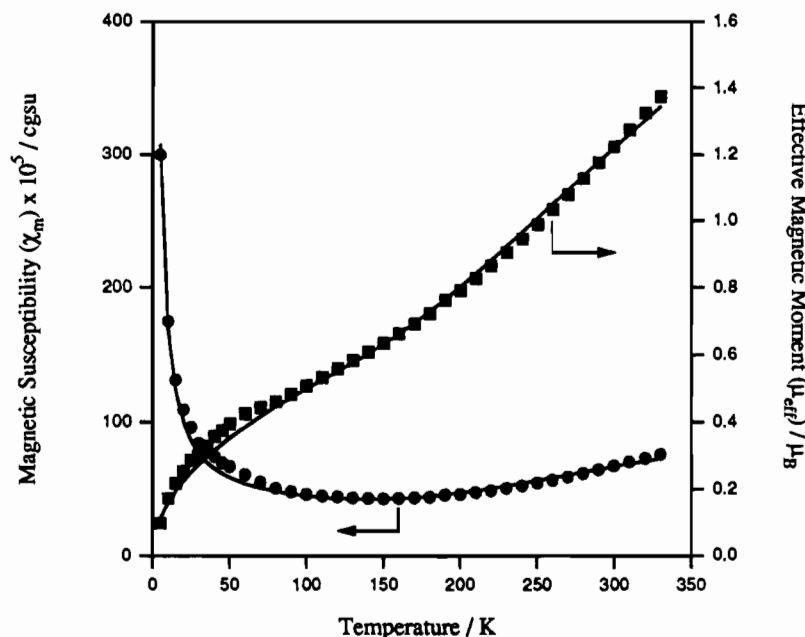
Figure 4. Plots of molar magnetic susceptibility (●) and effective magnetic moment (■) *versus* temperature for complex **4**. The shoulders in the data at *ca.* 50 K are artifacts due to liquid oxygen condensation on the sample (see Experimental Section). The solid lines are fits of the data to eq. 6; see the text for the fitting parameters.

amenable to additional investigation by variable-temperature magnetic susceptibility studies which can probe the population of the triplet state as a function of temperature. Further, the latter approach can provide an accurate determination of the true singlet–triplet energy gap in the molecule.

Magnetic Susceptibility Studies. Variable-temperature, solid-state magnetic susceptibility studies have been performed on powder samples of complex **4** in the temperature range 5.0–330 K (Figure 4). The effective magnetic moment per dinuclear complex, μ_{eff}/V_2, gradually decreases from 1.35 μ_B at 330 K to 0.095 μ_B at 5.0 K. The 330 K value corresponds to 0.96 μ_B/V, considerably less than the value expected for a magnetically-isolated V^{III} (d^2) ion (2.83 μ_B); it is also less than expected for a noninteracting V^{III} ion possessing only *one* unpaired electron (1.73 μ_B). The data thus show that the low value of μ_{eff} at room temperature decreases even further at lower temperatures and approaches zero at 5 K. This behavior is totally consistent with Figure 3, *viz* an $S = 0$ ground state and an $S = 1$ excited state that is thermally accessible.

Since the structural and MO calculations suggest the presence of a metal–metal single bond tying up two of the V d electrons in a relatively low-lying bonding orbital (*vide supra*), the best magnetochemical description of the complex is as two interacting $S = \frac{1}{2}$ metal ions; i.e., no $S > 1$ state being involved. A theoretical expression describing the molar magnetic susceptibility (χ_M/V_2) versus temperature dependence is provided by the Bleaney–Bowers equation (eq 6) based on the spin Hamiltonian

$$\chi_m = \frac{2Ng^2\mu_B^2}{kT}\left[\frac{1}{3+\exp 2x}\right](1-\varrho) + \frac{2\varrho Ng^2\mu_B^2}{3kT} + TIP \quad (6)$$

$\hat{H} = -2J\hat{S}_1\cdot\hat{S}_2$, where $x = -J/kT$, N is Avogadro's number, ϱ is the mole fraction of paramagnetic impurity (assumed to be mononuclear V^{III} and giving the second term in eq 6), TIP is the temperature independent paramagnetism, and the other symbols have their usual meaning.

The experimental data were least-squares fit to eq 6, and a satisfactory fit was obtained with $J = -355 \pm 20$ cm^{-1}, $g = 2.04$, TIP $= 300 \times 10^{-6}$ cm^3 mol^{-1}, and $\varrho = 0.014$; the solid lines in Figure 4 show this fit to the experimental χ_M data. Also

shown is a fit to the data plotted as μ_{eff} *vs* T. The singlet–triplet energy gap is thus $|2J| = 710$ cm^{-1} or approximately 0.09 eV. This may be compared with the $\sim$0.02 eV HOMO–LUMO gap from the EHT calculation; as stated earlier, the one-electron energies available from the MO calculation are not an accurate estimate of the true singlet–triplet gap in a multi-electron system, so that the observed degree of correspondence is quite satisfying. A value of 710 cm^{-1} for the singlet–triplet gap results in $\sim$9% of the molecules being in the $S = 1$ excited state at room temperature ($\sim$300 K).

There are few paramagnetic triply-bridged V^{III}_2 or V^{IV}_2 complexes known with which to magnetochemically compare complex **4**. The species [V$_2$O(OAc)$_2$(tacn)$_2$]$^{2+}$ (tacn = 1,4,7-trimethyl-1,4,7-triazacyclononane)[16] possesses a [V^{III}(μ-O)(μ-OAc)$_2$V^{III}] core and exhibits a strong *ferro*magnetic exchange interaction ($J > +200$ cm^{-1}) and a $S = 2$ ground state. On protonation of the bridging oxide to hydroxide,[32] the nature of the exchange interaction changes to antiferromagnetic with $J = -36$ cm^{-1}. Although these species contain a bridging oxygen (O^{2-} or OH$^-$), they are structurally and electronically very different from **4**. The latter possesses three monoatomic bridges, together with a close V··V separation (2.579(3) Å) and a V–V single bond. In contrast, [V$_2$O(OAc)$_2$(tacn)'$_2$]$^{2+}$ has one mono-atomic and two triatomic bridges and a V··V distance of 3.250-(2) Å, which precludes V–V bonding[16]; on protonation to the μ-OH$^-$ form, the V··V distance undoubtedly increases further.

(25) Bolinger, C. M.; Rauchfuss, T. B.; Rheingold, A. L. *J. Am. Chem. Soc.* **1983**, *105*, 6321.
(26) Bolinger, C. M.; Rauchfuss, T. B.; Rheingold, A. L. *Organometallics* **1982**, *1*, 1551.
(27) Herberhold, M.; Kuhnlein, M.; Schrepfermann, M.; Ziegler, M. L.; Nuber, B. *J. Organomet. Chem.* **1990**, *298*, 259.
(28) Sendlinger, S. C.; Nicholson, J. R.; Lobkovsky, E. B.; Huffman, J. C.; Rehder, D.; Christou, G. *Inorg. Chem.* **1993**, *32*, 204.
(29) Duraj, S. A.; Andras, M. T.; Kibala, P. A. *Inorg. Chem.* **1990**, *29*, 1232.
(30) Tiekink, E. R. T.; Yan, X. F.; Young, C. G. *Aust. J. Chem.* **1992**, *45*, 897.
(31) Halbert, T. R.; Hutchings, L. L.; Rhodes, R.; Stiefel, E. I. *J. Am. Chem. Soc.* **1986**, *108*, 6437.
(32) Knopp, P.; Wieghardt, K. *Inorg. Chem.* **1991**, *30*, 4061.

Protonated and unprotonated versions of the analogous tris-(pyrazolyl)borate complexes have also been recently reported.[17]

Perhaps more related to complex **4** is the $[V_2Cl_7(THF)_2]^-$ ion,[33] which contains a $[V_2(\mu\text{-Cl})_3]$ core and a V··V separation of 3.176(2) Å; it is antiferromagnetically coupled with $J = -48.1$ cm^{-1}. The V^{III}_2 (d^3/d^3) species $[V_2Cl_3(THF)_6][Zn_2Cl_6]$[34] also has a $[V_2(\mu\text{-Cl})_3]$ core, a V··V distance of 2.973(1) Å, and $J = -38$ cm^{-1}. Thus, as might have been predicted, the antiferromagnetic exchange interaction in **4** is significantly stronger than those in triply-chloride-bridged species, a difference that can be attributed primarily to the presence in **4** of the bridging oxide ion, the resultant short V−O bond lengths, and the metal−metal bond (and its decrease of the V··V separation).

Paramagnetic NMR Studies in Solution. Complex **4** is either only sparingly soluble or unstable in common organic solvents except THF, and d_8-THF was therefore employed for NMR investigations. Variable-temperature NMR studies in solution can be employed to determine the exchange parameter J of an exchange-coupled system or the singlet−triplet gap in weakly metal−metal bonded systems, and this can be used as an alternative or complementary method to solid-state magnetic susceptibility studies. A number of complexes have been investigated, such as oxide-bridged Fe^{III}_2 species[35] and metal−metal multiply-bonded dinuclear complexes.[36] This solution technique is necessarily limited to relatively high temperatures and therefore requires J to be large enough to give a significant change in the relative populations of the ground and thermally-accessible excited state(s) over the temperature range available. Haw and co-workers, however, have recently employed solid-state NMR data for the evaluation of J for copper(II) carboxylates in their solid form.[37]

For a dinuclear complex with one unpaired electron on each metal (the effective situation in complex **4**), the temperature dependence of an ^{1}H NMR peak is given by eq 7, where $x =$

$$\nu_{obs} = \nu_{dia} + \frac{4\pi g\mu_B \nu_o A}{\gamma_H kT}\left[\frac{1}{3 + \exp 2x}\right] \quad (7)$$

$-J/kT$, ν_{obs} is the resonance frequency, ν_{dia} is the resonance frequency of the same nucleus in an equivalent diamagnetic complex, A is the electron/proton hyperfine coupling constant (Hz), ν_o is the spectrometer frequency, and γ_H is the proton gyromagnetic ratio.[37,38] Equation 7 assumes that the paramagnetic shift ($\nu_{obs} - \nu_{dia}$) of a resonance from its diamagnetic position (ν_{dia}) is due to a contact shift mechanism, i.e., that dipolar shift contributions are zero or relatively minor.

The ^{1}H NMR spectrum of complex **4** in d_8-THF was complicated and displayed a large number (>10) of PhS$^-$ and Me$_2$bpy peaks in the $\delta = 0-12$ ppm region, consistent with effective C_2 symmetry in solution (14 peaks expected). Many of the peaks were broad and several were overlapping, making
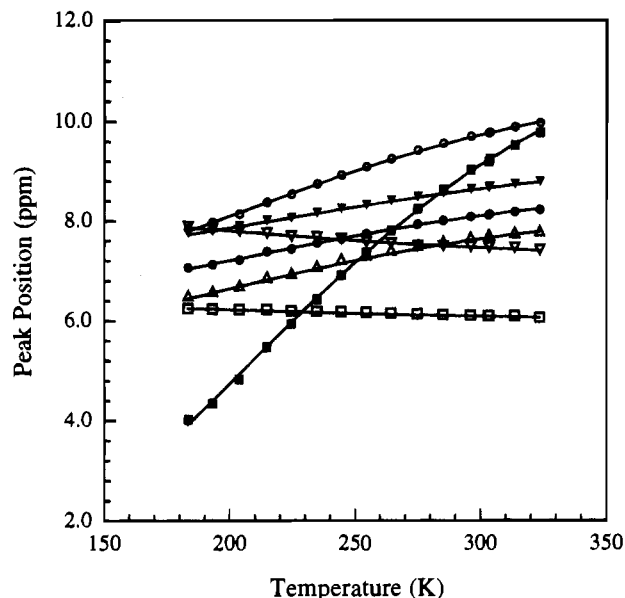
(33) Rambo, J. R.; Bartley, S. L.; Streib, W. E.; Christou, G. *J. Chem. Soc., Dalton Trans.* **1994**, 1813.

(34) Bouma, R.; Teuben, J. H.; Beukema, W. R.; Bansemer, R. L.; Huffman, J. C.; Caulton, K. G. *Inorg. Chem.* **1984**, *23*, 2715.

(35) (a) Boyd, P. D. W.; Smith, T. D. *Inorg. Chem.* **1971**, *10*, 2041. (b) Boyd, P. D. W.; Murray, K. S. *J. Chem. Soc. A* **1971**, 2711.

(36) (a) Cotton, F. A.; Chen, H.; Daniels, L. M.; Feng, X. *J. Am. Chem. Soc.* **1992**, *114*, 8980. (b) Cotton, F. A.; Eglin, J. L.; James, C. A.; Luck, R. L. *Inorg. Chem.* **1992**, *31*, 5308.

(37) (a) Campbell, G. C.; Haw, J. F. *Inorg. Chem.* **1988**, *27*, 3706. (b) Campbell, G. C.; Reibenspies, J. H.; Haw, J. F. *Inorg. Chem.* **1991**, *30*, 171.

(38) (a) Kurland, R. J.; McGarvey, B. R. *J. Magn. Reson.* **1970**, *2*, 286. (b) Boersma, A. D.; Phillippi, M. A.; Goff, H. M. *J. Magn. Reson.* **1984**, *57*, 197. (c) Holm, R. H.; Hawkins, C. J. In *NMR of Paramagnetic Molecules*; La Mar, G. N., Horrocks, W. DeW., Holm, R. H., Eds.; Academic: New York, 1973; Chapter 7.

Figure 5. Plots of VT ^{1}H NMR data for complex **4** in d_8-THF for the seven resonances that are resolved throughout the whole temperature range. The solid lines are fits of the data to eq 7; see the text and Table 8 for the fitting parameters.

peak assignments difficult, and they were therefore not attempted; it was in any case not necessary for our objectives. Variable-temperature data were collected in the range -90 to $+50$ °C. Only seven resonances remained clearly resolvable for reliable chemical shift measurement throughout this entire temperature range, and only these seven data sets were therefore employed in subsequent calculations.

Before an attempt was made to fit the data to eq 7, the question of dipolar shift contributions was addressed. For a complex such as **4**, the dipolar shift contribution (ν^{dip}_{obs}) to ν_{obs} is given by eq 8,[37,38] where r is the distance of the resonating

$$\frac{\nu^{dip}_{obs}}{\nu_o} = \frac{2\mu_B^2}{3kTr^3}(3\cos^2\theta - 1)(g_\perp^2 - g_\parallel^2)\left(\frac{1}{3 + \exp 2x}\right) \quad (8)$$

nucleus from the paramagnetic center (taken as the midpoint between the two metals) and θ is the angle between the V−V vector and the line connecting the resonating nucleus to the paramagnetic center. To estimate the ν^{dip}_{obs} values that might be occurring in the present case, we determined ν^{dip}_{obs} for $J = 0$ and $r = 3.0$ Å (estimated from the crystal structure to be approximately the shortest such value in the molecule). In addition, we employed the maximum $g_\perp^2 - g_\parallel^2$ (Δg^2) value we could find for non-vanadyl, six-coordinate V^{IV} (d^1) species in the literature ($g_\parallel = 1.931$, $g_\perp = 1.760$, $\Delta g^2 = 0.63$ for *cis*-$[VCl_2(phen)_2]^{2+}$).[39] In vanadyl species, Δg^2 is much smaller (0.02−0.05) as a result of the short, triple bond. Electronically, the pseudo-V^{IV} (d^1) metal centers in **4** are expected to be intermediate in character between a vanadyl and non-vanadyl species, and as such the value of 0.63 represents a reasonable upper boundary for Δg^2. Using these data, the estimated dipolar shifts were found to be small compared with the observed paramagnetic shifts; thus the latter were concluded to be dominated by contact shifts, and the use of eq 7 was deemed valid.

The seven data sets were separately fit to eq 7, and the results are shown in Figure 5. The fitting parameters were J, A, and ν_{dia}, and the fits are shown as solid lines. The fits can be seen

(39) Jezierski, A.; Barrie Raynor, J. *J. Chem. Soc., Dalton Trans.* **1981**, 1.

Table 8. Fitting Parameters[a] for the VT ^{1}H NMR Data[b]

peak no.[c]	J, cm^{-1}	A, MHz	ν_{dia}, ppm
1	-281 ± 5	2.45	6.79
2	-281 ± 5	6.60	1.22
3	-296 ± 5	1.24	7.32
4	-280 ± 7	1.34	6.48
5	-270 ± 7	1.45	5.74
6	-276 ± 7	-0.510	8.09
7	-280 ± 8	-0.205	6.33

[a] VT data were fitted to eq 7. [b] In d_8-THF. [c] Numbered according to decreasing chemical shift at +50 °C in Figure 5.

to be very good, and a listing of obtained J, A, and ν_{dia} values for the seven data sets is given in Table 8; the obtained values of J were in the -270 to -296 cm^{-1} range (average, -280 cm^{-1}). The J value of -280 ± 20 cm^{-1} and the resulting singlet–triplet energy gap of $|2J| = 560$ cm^{-1} is satisfyingly similar to the solid-state values (-355 and 710 cm^{-1}, respectively). The difference is undoubtedly due to the assumptions and approximations inherent in the two methods, and perhaps some real changes to J on dissolution of the complex as packing forces are relaxed and concomitant small changes to structural parameters occur, particularly the bridging angles. On the other hand, the overall similar values obtained from the solid-state and solution studies supports retention of the triply-bridged dinuclear structure of **4** on dissolution in THF. The excellent agreement between the experimental points and the behavior predicted by eq 7 also supports the validity of ignoring dipolar contributions to ν_{obs}.

Discussion

The use of monodentate PhS$^-$ in conjunction with the chelate bpy (or its derivatives) provides convenient access to soluble, discrete mononuclear V^{III} thiolate species. The latter provide excellent springboards to other V^{III} and V^{IV} complexes. In the present work, the high sensitivity of V^{III} thiolates to O$_2$ and H$_2$O is employed to our advantage by means of controlled aerial oxidation and hydrolysis reactions to introduce oxide ions with and without oxidation state changes, respectively. These reactions have yielded a number of new products, of which complex **4** is of particular interest. Its [M$_2$(μ-O)(μ-SPh)$_2$] core is novel for any metal, except for two distantly-related Mo species, and it provides a welcome new addition to the still only very small family of V^{III}/S complexes with V–V bonds.

The combination of X-ray crystallography, EHT calculations, VT solid-state magnetochemistry, and VT ^{1}H NMR studies has allowed the conclusion to be reached that **4** (a d^2–d^2 system) contains a V–V σ bond and that the remaining two d electrons occupy orbitals of δ symmetry that are weakly overlapping to yield δ and δ^* orbitals. Notwithstanding the involvement of bridging ligand orbitals in the σ bonding orbital, the description of **4** as containing a V–V single bond is considered valid. The δ overlap is very weak, however, and the two electrons may be considered to be essentially metal-localized. The δ-symmetry overlap does, nevertheless, provide a true nondegenerate pair

of δ and δ^* M.O.'s (again with bridging-ligand participation) which represent the source of the room-temperature paramagnetism of the molecule. From an M.O. viewpoint, the complex has a $\sigma^2\delta^2$ ($S = 0$) ground state and a low-lying $\sigma^2\delta^1\delta^{*1}$ ($S = 1$) excited state. Given the weak δ overlap, however, an alternative description, in magnetochemical parlance, is as a complex with a σ bond and two metal-based electrons that are antiferromagnetically-coupled *via* a superexchange mechanism involving the bridging ligands to give a singlet ground state and triplet excited state. Fitting of VT magnetic susceptibility data gives a value of J of -355 ± 20 cm^{-1}, a relatively large number that leads to a singlet–triplet energy gap $|2J|$ of 710 cm^{-1} and which thus rationalizes the only weak paramagnetism even at 330 K (0.96 μ_B/V). ^{1}H NMR data lead to a solution value of $|2J|$ that is similar to the solid-state value.

It is worth pointing out that we can choose to ignore (i) the crystallographic evidence for a V–V bonding interaction and (ii) the results of the EHT calculation indicating a low-lying σ-bonding orbital and thus treat the complex magnetochemically as a d^2/d^2 ($S = 1/S = 1$) dimer undergoing antiferromagnetic exchange interactions to give a spin manifold with total spins of $S = 0$, 1, and 2 with energies of 0, $-2J$, and $-6J$, respectively. This gives the same fit with the same value of J, since the $S = 2$ second excited state is $|4J| = 1420$ cm^{-1} above the $S = 1$ state and thus insignificantly populated even at room temperature; it does not therefore affect the observed χ_M vs T behavior. However, the description of **4** as an exchange-coupled d^2/d^2 dimer is not, in our opinion, a justifiable one, for the various reasons detailed in this paper. This is in contrast to our recent report on (NEt$_4$)[V$_2$Cl$_7$(THF)$_2$] where the V$\cdots$V separation of 3.176(2) Å was interpreted as precluding V–V bonding, and the magnetochemical data were therefore analyzed on the basis of an $S = 0$, 1, 2 spin manifold.[33]

The combined results lead to a satisfyingly consistent picture of complex **4** as containing two distinct types of electron–electron interactions *viz.* "metal–metal bonding" and weaker magnetic exchange interactions. With the results on **4** at hand, our attention is now turned toward other V$_2$ species that appear to contain a similar electronic makeup. VT magnetic susceptibility studies have now been completed on (NEt$_4$)$_2$[V$_2$(edt)$_4$], for example, and the results will be reported in due course. In addition, further reactivity studies on discrete V^{III}/PhS$^-$ species have yielded more new V$_x$ complexes, and these results will also be the subjects of future reports.

Supplementary Material Available: Textual and tabular summaries of the structure determination, tables of atomic coordinates, thermal parameters, and bond distances and angles, and figures with atom numbering for complexes **2** and **4** (25 pages). Ordering information is given on any current masthead page.

IC941172Y